Infrared Focal Plane Array Imaging System Characterization by Means of a Blackbody Radiator

Francisca Parra[1,2,3], Pablo Meza[1,2], Carlos Toro[1,2], and Sergio Torres[1,2]

[1] Departamento de Ingeniería Eléctrica, Universidad de Concepción, Casilla 160-C, Concepción, Chile
[2] Center for Optics and Photonics, Universidad de Concepción, Concepción
[3] Aeronautical Polytechnic Academy Chilean Air Force Santiago, Chile

Abstract. Infrared (IR) Focal plane array (IRFPA) cameras are nowadays both, more accessible and with a broad variety in terms of detectors design. In many cases, the IRFPA characterization is not completely given by the manufacturer. In this paper a long wave 8-12 [μm] microbolometer IRFPA is characterized by means of calculating the Noise Equivalent Temperature Difference (NETD) and the Correctability performance parameters. The Correctability parameter has been evaluated by using a black body radiator and Two-Points calibration technique. Also, the Transfer Function of the microbolometer IR camera has been experimentally obtained as well as the NETD by the evaluation of radiometric data from a blackbody radiator. The obtained parameters are the key for any successful application of IR imaging pattern recognition.

1 Introduction

Currently, the development of IR imaging sensors have been such that the market has been flooded with different types of IR cameras, each one with different features as presented in [1]. The main difference between these cameras is in the sensor type used for detecting the infrared radiation.

Depending on the interaction nature between the detector material and the IR radiation, the photo-detectors are classified on intrinsic, extrinsic, photoemissive, and quantum well detectors [2]. The second class of IR detectors is composed by thermal detectors, where the incident radiation is absorbed and it changes the material temperature, that change modifies some physical properties as resistivity to generate an electrical signal output.

In contrast to photo-detectors, the thermal detectors typically operate at room temperature. One of the most popular thermal detectors is the amorphous silicon (a-Si) microbolometer as presented in [3] and as any detector, they are affected by many type of noise sources.

In spite of the the first bolometer was designed in 1880, according to [4], the development release to this technology was under classify military contacts, so

C. San Martin and S.-W. Kim (Eds.): CIARP 2011, LNCS 7042, pp. 105–112, 2011.

the public according to this in 1992 were surprising in the worldwide infrared community, and they are still object to several research.

To apply a IR microbolometer camera to IR imaging application a fully characterization of the detector noise is needed. Inherent to this kind of equipments is the Fixed Pattern Noise (FPN); it can be defined as a fixed noise superimposed over the IR image. The FPN is generated by the nonuniform response of the neighbors detectors for the same integrated IR irradiance. Several methods have been developed to eliminate this undesired effect, with different results and operations conditions, some of them are compared in [5].

In [6] and [7] it is shown the importance to have a good understanding of the detectors response. This can be achieve by using a thermal reference known as a blackbody [8], which is a laboratory equipment capable of delivering a flat input temperature. Having this in consideration, many FPA parameter such that radiometric curves, NETD, Correctability, etc., can be calculated using this equipment, as it is presented in [9] and [10].

The present study deals with three laboratory characterization parameters evaluated for a CEDIP Jade Uncooled (UC) camera, long wave 8-12 [μm] microbolometer IRFPA. This paper is organized as follows: In section 2, the radiometric curve, the NETD, and the Correctability parameters are defined. In section 3 the experimental technique to perform an evaluation of such parameters is described and the main results are shown. Finally, the most important conclusions are detailed on section 4.

2 Parameters

In this section, the three parameters under analysis are presented. They are able to represent different characteristics of an IR imaging system. Note that they are interdependent, because as it will be shown, the radiometric analysis gives the basis to perform the NETD and the Correctability analysis.

2.1 Radiometric Transfer Function

For measurements of radiometric parameters, the experimental setup use a blackbody calibration source, whose temperatures radiance can be accurately calculated, and the IRFPA imaging system to be evaluated. The blackbody is composed by a plate with a roughened surface covered with a high emissivity painting. The uniform temperature surface can be stabilized in a time lower than 10 minutes with an emissivity average of 0.95.

This equipment is essential to perform the IRFPA System Transfer Function (SiTF). It is estimated by the measure of several flat inputs at different temperature radiation, which are controlled by the blackbody source. The data acquired can be represented as a Data Cube, because there exists information on three dimensions, two spatial axes and one temporal axe. The measures resulted must be averaged, and then the SiTF is determined [11]. It is typically represented in response units of voltage, digital counts, etc. vs units of the source such as

temperature, flux, etc. Therefore, any digital value can be associated to a specific input temperature.

According to this behavior, at a frame n^{th}, a general model for each ij detector in the FPA is often described by a linear relationship between the incoming irradiance $X_{i,j}(n)$ and the readout data $Y_{i,j}(n)$ as follows:

$$Y_{i,j} = A_{i,j}X_{i,j} + B_{i,j} \tag{1}$$

The SiTF, can be used also to determine how is increased the signal detected regarding the input, and to determine the sections in which it can be approached to the first order model described in the equation 1. In a Two-Point or Multipoint correction method, this is particularly important because it will indicate the range for which the method is more accurate to apply.

2.2 Noise Equivalent Temperature Difference, NETD

The NETD is a performance metrics to measure the IRFPA thermal resolution, as it is mentioned in [12], it is the smallest difference in a uniform temperature scene that the FPA can detect. According to [13], the typical value for a microbolometer is on the order of 100 [mK]. Note that the knowledge of such parameter is crucial for IR pattern recognition. Further, the NETD parameter measures the system's ability to perceive targets with a low thermal contrast with the imaging background. It can be defined as the ratio between the noise rms inherent on the system and the SiTF, then:

$$NETD = \frac{N_{rms}[volts]}{SITF_{Slope}[volts/K]} \tag{2}$$

2.3 Correctability

There are several methods to calibrate IR imaging system. The foregoing, has generated the need of IR image quality indexes to evaluate the quality of the applied correction method.

The Correctability figure of merit is based on the use of a thermal reference (blackbody source). Further, the Correctability is able to evaluate the mitigation of the FPN after calibration. Moreover this parameter magnitude is proportional to the rate within the total noise and the temporal noise. Mathematically, it is defined by:

$$c = \sqrt{\frac{\sigma^2_{total}}{\sigma^2_v} - 1} \tag{3}$$

where σ^2_{total} is the spatial variance given by:

$$\sigma^2_{total} = \frac{\sum_{j=1}^{n}(Y_j^c - \overline{Y})^2}{n-1} \tag{4}$$

Y_j^c is the j^{th} corrected pixel value, $\overline{Y}$ is the spatial sample mean of the uncorrected frame, and n is the number of pixels on the FPA.

Note that a Correctability value $c = 0$ indicates that the FPN has been completely removed, which is highly desired. If the value is $c = 1$, the FPN after the correction equals the temporal noise. When the level of correction is poor, the residual FPN exceeds the values of the temporal noise, achieving c values greater than 1.

3 Experimental Setup and Data Processing

To measure, experimentally, the IR imaging parameters outlined above, a laboratory set up has been implemented. This is composed by a CEDIP Jade UC FPA Camera with a spatial resolution of 240×320 pixels, a spectral response between 8-12 [μm], 14 bits digital output. Further, detector material is an uncooled a-Si microbolometer. For this system, the manufacturer guaranties a NETD lower than 100 [mK]. The reference IR source used is a blackbody radiator, which operates between 0-150 [°C] and with a thermal resolution of 0.1 [°C].

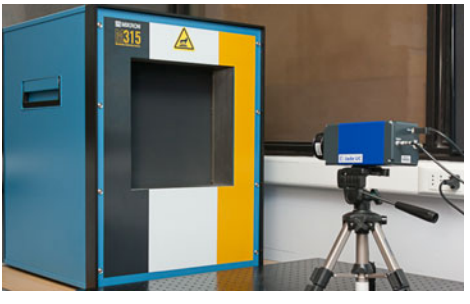

Fig. 1. Laboratory Setup

3.1 Radiometric Procedure

To measure the SiTF, 300 IR imaging frames where captured for each blackbody setup temperature. Furthermore, the integration time of the IR imaging system is fixed at 60 μs. Therefore, the dimensions for each data cube are $240 \times 320 \times 300$. In this case, there have been implemented measures between 0 and 150[°C] with 5°[C] incremental between the IR imaging frames. The average of each data cube was plotted and it is represented by the Fig. 2.

Note that on Fig. 2 the standard deviation of each data cube decreases as long as the temperature increases.

With the experimental data a linear regression, in the least squares sense, was performed over all the image's dynamic range. However because of the nonlinearity of the imaging system response to the blackbody radiator, a linear regression by sections is required. Further, the dynamic range has been separated on three

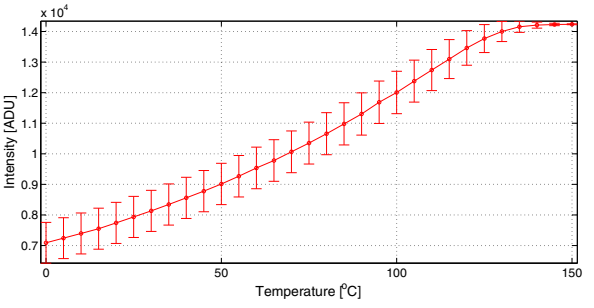

Fig. 2. Transfer Function CEDIP Camera

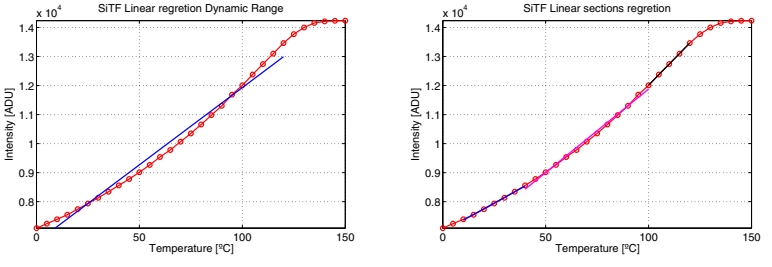

Fig. 3. SiTF Linear regression

sections representing the low, medium and high temperature values. The above procedure can be seen in Fig. 3.

It can be seen in Table 1 the First-Order parameter obtained after the linear regression for each range. Note that the slope is growing from the first section to the third one.

Table 1. First-Order parameter of the radiometric procedure

[T. Range [°C]	$\overline{A}_{i,j}$ [ADU/°C]	$\overline{B}_{i,j}$ [ADU]
[10 , 40]	39.1	6973.7
[40 , 100]	57.5	6128.8
[100 , 120]	72.7	4741.3

3.2 NETD Experimental Procedure

The NETD must be calculated at different levels of temperature, because the slope obtained by linear regression is growing along with the temperature levels. Therefore, the steps to perform the NETD can be numbered as follows:

1. A temporal noise estimation is calculated for each specific temperature in the linear range.

2. A temporal IR imaging frame average at each temperature is calculated.
3. To isolate the temporal component in one frame, the difference between the particular frame and the previous averaged frame is obtained. This procedure is repeated for each frame in the chosen data cube.
4. Now it is calculated the rms value of the previous obtained frame.
5. Calculate the standard deviation for each pixel along the temporal axis and then the final frame is averaged, see Fig. 4 for a best understanding.

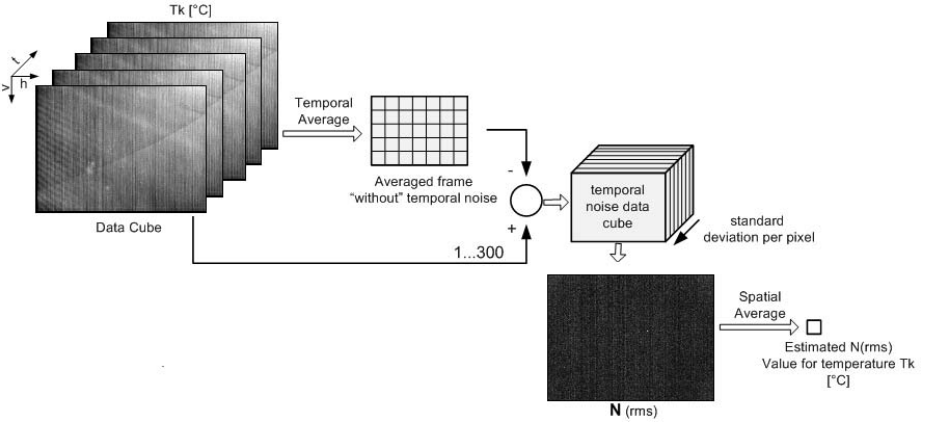

Fig. 4. Temporal Noise Procedure

The results are detailed on Table 2. It is appreciated a NETD value decrease as the temperature is higher. Furthermore, it shows that the NETD is not constant for all the temperatures. According to this, it is possible to say that the thermal resolution is better when the target temperature is higher.

Table 2. NETD experimental result at different temperature ranges

T. Range [°C]	T. Selected [°C]	SiTF [a.u/mK]	N(rms)[a.u.]	NETD [mK]
[10 , 40]	20	39.1	3.71	95.0
[40 , 100]	70	57.5	4.08	70.9
[100 , 120]	110	72.7	4.77	65.6

3.3 Correctability Experimental Procedure

To evaluate the Correctability IR imaging performance parameter, it is necessary to perform a FPN correction on the raw IR imaging obtained by using the experimental setup shown in Fig. 1. A Two-Point correction has been implemented, retrieving the correction parameters for different ranges of temperature $[T_{min}, T_{max}]$. The corrupted video set is selected by taking a temperature image between the $[T_{min}, T_{max}]$.

The procedure steps to calculate the Correctability can be enumerated as follow:

1. Select the raw IR frame and its corresponding calibrated frame over which the Correctability will be calculated.
2. Calculate the spatial sample variance σ^2_{total}, given by the equation 4, over the two previous frames.
3. Calculate the temporal variance σ^2_v.
4. Finally, apply the equation 3 to evaluate the Correctability parameter.

Note that this steps can be replicated to any FPN calibration method. The results shown in Table 3 indicate that the correction with the poorest performance happened for the widest temperature range. This result is expected due to the low accuracy of the linear approximation in broad ranges.

Table 3. Correctability performance parameters at six different temperatures, each one tested with a different Two-Point correction

$[T_{min}, T_{max}]$°C at T°C	Correctability
[25 , 45] measured at 35	0.6581
[60 , 80] measured at 70	0.6733
[95 , 115] measured at 105	23.4465
[20 , 30] measured at 25	0.5858
[10 , 140] measured at 75	94.2718

4 Conclusions

In this paper, three IR imaging system parameters have been analyzed by means of a laboratory characterization. This has been achieved by using a CEDIP Jade UC IRFPA camera and a Mikron blackbody radiator.

The radiometric transfer function coming out to be nonlinear up to 100 [°C] and down to 20 [°C]. Further, the linear operation range was determined to be between the previous values. Such linear range justifies the potential to apply the JADE camera to most of the imaging applications in the field of human biometrics.

The calculated NETD values are consistences with the ones delivered by the manufacturer. Further, the best NETD obtained was 65 [mK], which is a acceptable value for human biometrics IR pattern recognition.

Finally, the IR Correctability performance values obtained for two-points correction method, corroborate the figure of merit behavior according to the accuracy of the correction. The best value obtained was 0.59, which represent a correction below the electronic temporal noise.

As a general conclusion, it is necessary to say that the IR microbolometer technology is very noisy for IR pattern recognition and special performance parameters computations are necessary for any particular application.

Acknowledgements. This work was partially supported by Programa de Financiamiento Basal grant PFB08024. Pablo Meza and Carlos Toro are supported by a CONICYT PhD Scholarship. Sergio Torres is supported by Fondo Nacional de Desarrollo Científico y Tecnológico (FONDECYT) 1100522. Francisca Parra is also supported by the Aeronautical Polytechnic Academy Chilean Air Force.

References

1. Scribner, D.A., Kruer, M.R., Killiany, J.M.: Infrared focal plane array technology. Proceedings of the IEEE 79, 66–85 (1991)
2. Rogalski, A.: Infrared detectors: an overview. Infrared Physics and Technology 43, 187–210 (2002)
3. Vedel, C., Martin, J.L., Ouvrier-Buffet, J.L., Tissot, J.L., Vilain, M., Yon, J.J.: Amorphous silicon based uncooled microbolometer IRFPA. In: SPIE Conference on Infrared Technology and Applications XXV, Orlando, vol. 3698 (1999)
4. Rogalski, A.: Infrared Detectors, 2nd edn. Taylor & Francis, Boca Raton (2011)
5. Vera, E., Meza, P., Torres, S.: Total variation approach for adaptive nonuniformity correction in focal-plane arrays. Opt. Lett. 36, 172–174 (2011)
6. Dantes, D.: Characterization of infrared detectors for space applications. In: SPIE Detectors, Focal Plane Arrays, and Applications, vol. 2894, pp. 180–186 (1996)
7. Yon, J.J., Mottin, E., Biancardini, L., Letellier, L., Tissot, J.L.: Infrared microbolometer sensors and their application in automotive safety. In: Advanced Microsystems for Automotive Applications, pp. 137–157 (2003)
8. Mikron Infrared: Calibration Sources, `http://www.mikroninfrared.com/EN/products/calibration-sources/`
9. Schulz, M., Caldwell, L.: Nonuniformity correction and correctability of infrared focal plane arrays. Infrared Physics and Technology 36, 763–777 (1995)
10. Torres, S., Hayat, M., Armstrong, E.: On the Performance Analysis of a Recent statistical algorithm for non-uniformity correction in focal-plane arrays. In: Proc. CISST, vol. 3703 (2000)
11. Perconti, P., Zeibel, J., Pellegrino, J., Driggers, R.: Medical Infrared Imaging, pp. 4-1–4-10 (July 2007)
12. Vandervelde, T.E., Lenz, M.C., Varley, E., Barve, A., Shao, J., Shenoi, R.V., Ramirez, D.A., Jan, W., Sharma, Y.D., Krishna, S.: Quantum Dots-in-a-Well Focal Plane Arrays. IEEE Journal of Selected Topics in Quantum Electronics 14(4), 1150–1161 (2010)
13. Laveigne, J., Franks, G., Sparkman, K., Prewarski, M., Nehring, B., McHugh, S.: LWIR NUC Using an Uncooled Microbolometer Camera. In: Technologies for Synthetic Environments: Hardware-in-the-Loop Testing XV. Proceedings of the SPIE, vol. 7663 (2010)